Journal of Molecular Structure 1161 (2018) 433–441

Contents lists available at ScienceDirect

Journal of Molecular Structure

journal homepage: http://www.elsevier.com/locate/molstruc

Synthesis of 2-(bis(cyanomethyl)amino)-2-oxoethyl methacrylate monomer molecule and its characterization by experimental and theoretical methods

E.B. Sas [a, *], N. Cankaya [b], M. Kurt [c]

[a] Technical Sciences Vocational Schools, Ahi Evran University, Kırsehir, Turkey
[b] Department of Chemistry, University Usak, Usak, Turkey
[c] Department of Physics, Ahi Evran University, Kırsehir, Turkey

ARTICLE INFO

Article history:
Received 17 October 2017
Received in revised form
25 January 2018
Accepted 30 January 2018
Available online 16 February 2018

Keywords:
DFT
FT-Raman
FT–IR
NMR

ABSTRACT

In this work 2-(bis(cyanomethyl)amino)-2-oxoethyl methacrylate monomer has been synthesized as newly, characterized both experimentally and theoretically. Experimentally, it has been characterized by FT-IR, FT-Raman, ^{1}H and ^{13}C NMR spectroscopy techniques. The theoretical calculations have been performed with Density Functional Theory (DFT) including B3LYP method. The scaled theoretical wavenumbers have been assigned based on total energy distribution (TED). Electronic properties of monomer have been performed using time-dependent TD-DFT/B3LYP/B3LYP/6–311G++(d,p) method. The results of experimental have been compared with theoretical values. Both experimental and theoretical methods have shown that the monomer was suitable for the literature.

1. Introduction

Acrylates and its derivatives are soluble in alcohol, ether, and most organic solvents. There are various acrylates and acrylate derivatives that are commercially available. There are many studies about acrylates that have been originally synthesized in the literature -such as this one- and it is likely that there will be many more too [1]. There are widespread and common applications of methacrylate mono/polymers from glazing to lighting housing, bath tubs to structural adhesives place them within the most important commercial mono/polymers. The key to the success of these mono/polymers is that they produce a wide variety of structures in the versatility of acrylic monomers. This gives the ability of tailoring them to obtain the desired properties. Recently, mono/polymers based on amino methacrylate have attracted attention [2]. Different amino methacrylate monomers are used in a wide range such as waste water purification, polymeric membranes, solid phase extraction, chromatographic supports appropriate, biochemical sensors, drug delivery systems, protein purification and recovery, and such that. Recent years have also added value to NMR spectroscopy in the analysis of monomer/polymer, which lets evaluation of composition [3–6].

In this paper we discuss chemical and physical characterization of a new synthesized molecule. The aim of this study is to investigate the experimental effects of FT-IR, FT-Raman, ^{1}H and ^{13}C NMR and theoretical effects of Density Functional Theory (DFT) method on CMA2OEM. The spectroscopic attitude, geometric structure, electronic properties and thermodynamic properties of 2-(bis(cyanomethyl)amino)-2-oxoethyl methacrylate molecule were investigated with DFT/B3LYP method and 6–311++G(d,p) basis set. Infrared and Raman spectra were calculated and vibrational assignments were based upon total energy distributions (TED). ^{1}H, ^{13}C NMR spectra were recorded in $CDCl_3$ and compared with theoretically obtained spectra. Additionally, frontier molecular orbital analyses were also carried out for CMA2OEM. Besides, to obtain total density of states (TDOS or DOS) the partial density of states (PDOS) and overlap population density of states (OPDOS) spectra of molecule were used by GaussSum 2.2 [11].

* Corresponding author.
E-mail address: baburemine@gmail.com (E.B. Sas).

https://doi.org/10.1016/j.molstruc.2018.01.088
0022-2860/

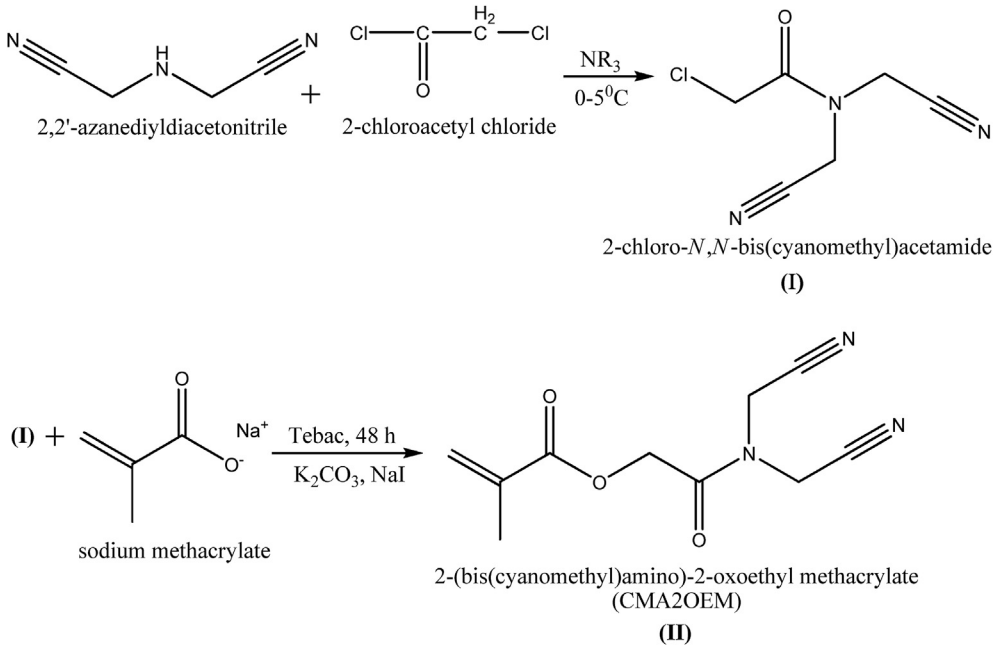

Fig. 1. (I) Synthesis of the 2-chloro-*N*,N-bis(cyanomethyl)acetamide (II) Synthesis of the 2-(bis(cyanomethyl)amino)-2-oxoethyl methacrylate (CMA2OEM).

2. Experimental

2.1. Synthesis of 2-(bis(cyanomethyl)amino)-2-oxoethyl methacrylate (CMA2OEM)

2,2′-Azanediyldiacetonitrile, Na^+methacrylate, $(Et)_3N$, chloroacetyl chloride, and triethyl benzyl ammonium chloride as a phase transfer catalyst were used as received. In order to synthesized 2-chloro-*N*,N-bis(cyanomethyl)acetamide, 2,2′-Azanediyldiacetonitrile and $(Et)_3N$ were dissolved in acetonitrile at 0–5 °C, and then chloroacetyl chloride was added dropwise. The reaction was stirred at 24 hours-500 rpm. The solution was filtered to remove the formed salt, crystallized to remove impurities. A viscous product was obtained (yield 82%). The reaction scheme is indicated in Fig. 1(I). 1 mol 2-choloro-*N*,N-bis(cyanomethyl)acetamide, 1.2 mol sodium methacrylate, phase transfer catalysts and hydroquinone as inhibitor dissolved in acetonitrile, the reaction was stirred at 85 °C for 24 h. At the end of the reaction period, the substance was filtered to remove the salt. It was washed with 5% NaOH base solution and removed from hydroquinone. Synthesis of original monomer is shown in Fig. 1(II).

FT-IR spectra was taken with Perkin Elmer Spectrum Two (UATR) IR spectrophotometer. Thermo Scientific Nicolet 6700 FT-IR/NXR FT-Raman Modül instrument using 1064 nm excitation from an Nd:YAG laser was used and measured in between of 4000-0 cm^{-1}. ^1H and ^{13}C NMR spectra were recorded on a Bruker 400 MHz spectrometer at room temperature in $CDCl_3$.

3. Computational details

The molecular geometry of CMA2OEM was optimized by DFT/B3LYP methods by using B3LYP/6–311G++(d,p) basis set. The vibrational bands were obtained with same basis set. Theoretical vibrational bands from 4000 to 1700 cm^{-1} and lower than 1700 cm^{-1} are scaled with 0.958 and 0.953 for B3LYP/6–311G++(d,p) basis set, respectively [7]. The vibration bands are assigned on the basis of TED performed with SQM program [8]. The electronic properties of CMA2OEM were obtained by TD-DFT method [9]. HOMO-LUMO was calculated at the same level with theoretical value. The ^1H and ^{13}C NMR chemical shifts were computed at the B3LYP/CC-pVDZ level of the gas state by using

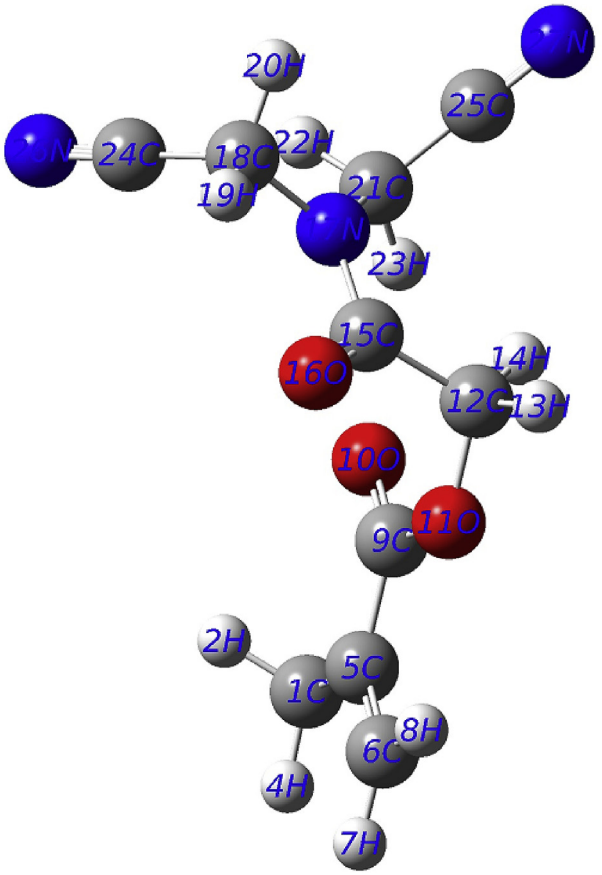

Fig. 2. Theoretical optimized geometric structure of the CMA2OEM.

Table 1
Selected geometrical parameters optimized in CMA2OEM [bond length (Å) and bond angle (°)].

Bond Length		Bond Angle	
C1–C5	1.50	C6–C5–C9	120.7
C6–H7	1.08	C5–C9–O11	114.0
C9–O10	1.21	C12–C15–O16	119.4
C15–O16	1.22	C15–N17–C18	117.7
C15–N17	1.38	C15–N17–C21	125.0
N17–C18	1.46	C18–N17–C21	117.2
N17–C21	1.46	N17–C18–H19	107.7
C24–N26	1.15	N17–C18–H20	110.0
C25–N27	1.15	H22–C21–H23	105.9

GIAO approach [10] and the values were referenced to TMS, which was computed at the same level with theoretical value. The TDOS, PDOS, and OPDOS density of states were computed using Gauss-Sum 2.2 program [11]. The calculations were carried out using GAUSSIAN09 [12] software.

4. Results and discussion

4.1. Characterization of 2-(bis(cyanomethyl)amino)-2-oxoethyl methacrylate (CMA2OEM)

The theoretical calculations of CMA2OEM were computed with DFT/B3LYP/6–311++G(d,p) level, and given in Fig. 2. Geometrical parameters of the title molecule are given in Table 1. In CMA2OEM, the bond lengths were computed N17–C18, N17–C21 as 1.46 Å and C24≡N26, C25≡N27 as 1.115 Å. While C9=O10 bond lengths were calculated at 1.21 Å, but C15 = O16 bond lengths were calculated 1.22 Å.

Some internal bond angles of the title molecule as C18–N17–C21 and C15–N17–C18 (117°) are smaller than bond angle as C15–N17–C21 (125°). This may be because of attached oxygen atom in C15 atom from interaction with O16.

4.2. Vibrational spectral analysis

FT-IR and Raman spectrums of compound were obtained using 6–311++G(d,p) basis set by DFT method. Theoretical and experimental FT-IR and Raman spectrums are shown in Fig. 3. All band assignments are presented in Table 2. CMA2OEM has 27 atoms and 75 vibrational modes. Vibrational bands were studied with TED. In this study, the wavenumbers from 4000 to 1700 cm and lower than 1700 cm are scaled with 0.958 and 0.953 for B3LYP/6–311G++(d,p) basis set, respectively. The correlation graphic of the theoretical and experimental bands for the compound was drawn and was shown in Fig. S1.

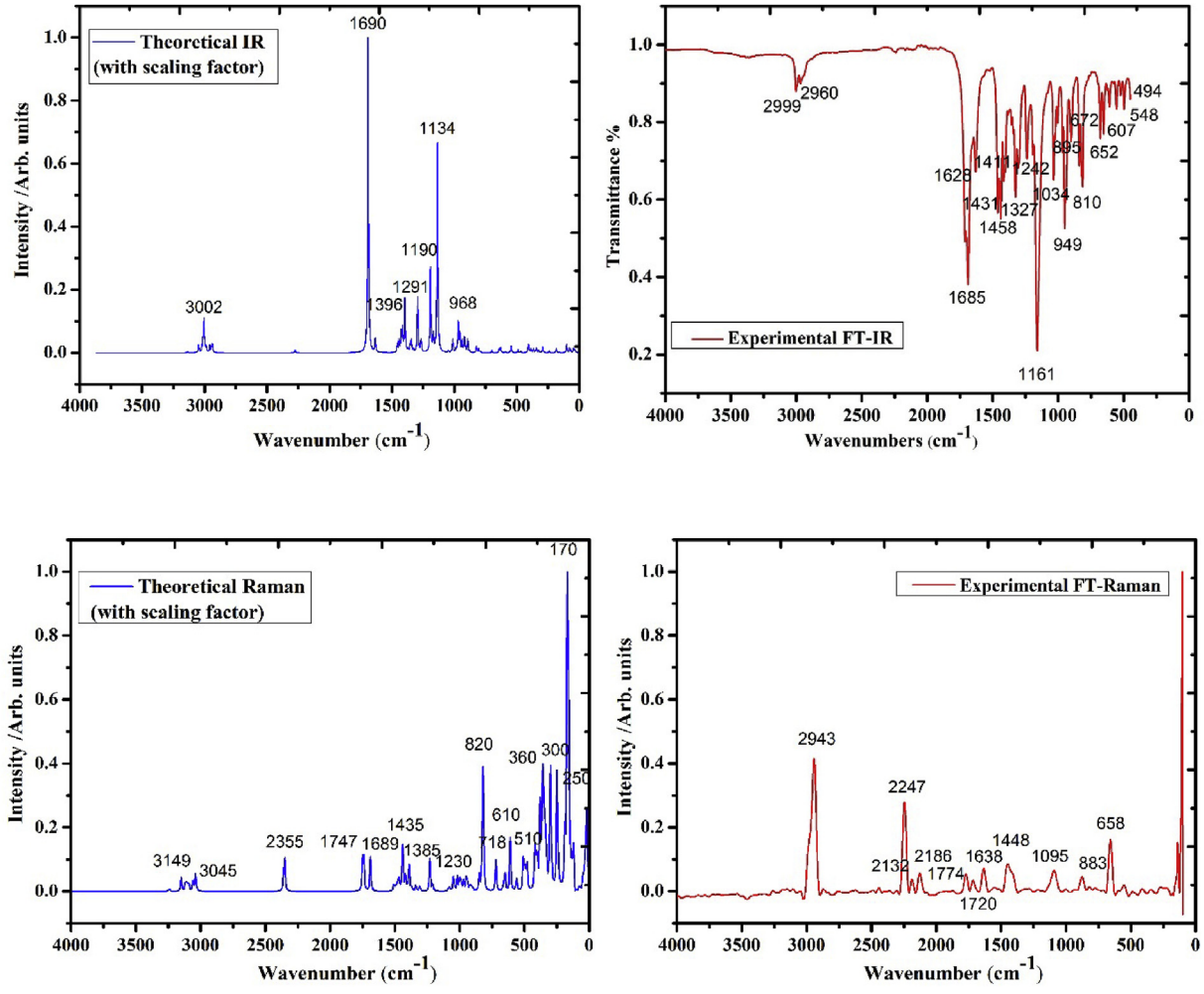

Fig. 3. The experimental and calculated (with the scale factor) FT-IR and FT-Raman spectra of the CMA2OEM.

Table 2
Comparison of the calculated and experimental vibrational spectra and proposal assignments of CMA2OEM molecule.

No	Experimental wavenumber		Theoretical wavenumber				TED (<10%)
	FT-IR	FT-Raman	Scaled	I_{IR}	S_{Ra}	I_{Ra}	Assignments[a]
1			21	0.67	4.28	0.41	τCCOC(74)
2			30	1.28	2.05	0.14	τCCOC(29)+τCCNC(49)
3			36	4.65	1.73	0.10	τCCNC(68)
4			46	4.10	1.23	0.05	τCCOC(10)+τCCCN(63)
5			47	2.57	1.89	0.08	τCCCO(77)
6			69	2.26	0.44	0.01	τCCCN(50)
7			78	7.57	1.09	0.03	τCCOC(40)+τCCNC(17)
8			103	14.63	0.69	0.01	τCCOC(34)+τCCNC(15)
9			162	0.45	0.31	0.00	τCCCH(93)
10			167	0.65	2.02	0.02	δCCC(52)
11			189	7.71	0.30	0.00	δCCC(61)
12			248	3.13	1.46	0.92	δCCO(46)
13			295	0.46	0.78	0.33	δCCO(34)+ δCNC(10)
14			302	10.05	1.66	0.68	δCCN(62)
15			336	4.43	1.69	0.55	δCCC(66)
16			355	8.50	3.43	1.00	δCCC(12)+τNCCH(24)+τCOCH(12)
17			363	1.18	1.61	0.45	δCNC(52)+τNCCH(10)+τNCCN(15)
18			378	6.73	2.17	0.55	δOCO(16)+τCCCC(26)
19			398	6.36	0.88	0.20	δCNC(13)+τCCCC(24)+τNCCN(10)
20			414	4.01	1.44	0.30	δCCC(31)
21			421	14.41	0.90	0.18	δCNC(20)+τCOCH(12)+τNCCN(18)
22	494		484	2.78	2.17	0.32	νCN(13)+δCCN(23)
23			506	6.10	3.08	0.42	δCCO(51)
24	548		563	12.50	1.03	0.11	δCCO(33)+τCOCH(10)+τCNCO(14)
25	607		610	1.53	3.63	0.32	νCC(25)+δOCO(36)
26	652	658	650	9.27	1.36	0.10	τCCCH(62)+τCOCO(23)
27	672		663	6.16	0.81	0.06	δCCN(47)
28			722	3.99	3.96	0.24	νCN(10)+τCNCO(19)
29	810		820	1.91	17.25	0.77	νCN(10)+τCNCO(17)
30			831	6.32	2.36	0.10	τCCCH(13)+τCOCO(37)+τCCCC(12)
31			851	11.78	2.61	0.11	τCOCO(16)
32	895	883	905	2.42	1.78	0.06	νCC(46)
33			923	24.07	1.46	0.05	νCC(58)+δCCN(10)
34			941	5.71	1.87	0.06	νCC(49)+δCCH(23)
35	949		951	26.56	2.71	0.08	νCC(32)+νCN(23)
36			969	20.31	2.28	0.07	δCCH(11)+τCOCH(15)+τCNCN(46)
37			988	33.62	3.02	0.09	τCCCH(98)
38			1001	53.85	3.04	0.08	νCO(22)+δCCH(13)
39			1018	7.03	4.43	0.12	δCCH(23)+τCCCH(23)
40	1034		1047	24.13	5.48	0.14	νCO(38)+τCCCH(24)
41			1072	0.12	0.34	0.01	δCHH(20)+τCCCH(75)
42		1095	1085	2.86	2.37	0.05	νCC(10)+δCCH(14)
43	1161		1173	379.43	0.24	0.00	νCO(37)+δCCH(12)+δOCO(12)
44			1208	29.22	3.51	0.06	νCN(43)+δCCH(28)
45	1242		1231	150.53	14.57	0.24	νCN(18)+δCCH(30)
46			1306	8.05	1.74	0.02	νCN(14)+δOCH(11)+ δCCH(33)+ τCNCH(10)
47			1310	17.76	1.52	0.02	δOCH(50)
48	1327		1338	99.60	4.25	0.06	νCC(36)+δCCH(14)
49			1373	6.14	3.18	0.04	δCHH(11)+ τCNCH(49)
50			1390	20.94	15.26	0.18	τCNCH(56)
51			1400	11.42	2.05	0.02	τCOCH(51)
52	1411		1418	5.74	13.03	0.15	δCHH(85)
53	1431		1440	7.99	26.88	0.29	δCHH(64)
54		1448	1443	90.75	5.50	0.06	νCN(19)+δCHH(39)
55	1458		1463	40.79	2.75	0.03	δCHH(61)+ δCCH(10)
56			1474	17.82	4.70	0.05	δCHH(66)+ τCCCH(22)
57			1474	17.26	14.20	0.15	δCHH(61)
58			1492	20.55	3.39	0.03	δCHH(68)+ τCCCH(21)
59			1506	14.54	9.53	0.09	δCHH(75)
60	1685	1638	1688	24.01	43.60	0.31	νCC(69)+δCHH(10)
61		1720	1744	56.58	68.65	0.44	νCO(81)
62		1774	1748	540.08	30.07	0.19	νCO(82)
		2132					Overtone combination
		2186					Overtone combination
63		2247	2353	2.82	127.17	0.33	νCN(91)
64			2356	2.24	96.65	0.25	νCN(92)
65	2960	2943	3038	12.14	150.87	0.16	νCH(98)sm
66	2999		3042	6.79	91.82	0.09	νCH(97)sm
67			3058	13.06	131.81	0.13	νCH(83)sm
68			3090	9.08	58.28	0.06	νCH(97)asm
69			3097	3.78	75.50	0.07	νCH(93)asm
70			3107	57.54	112.46	0.11	νCH(88)asm

Table 2 (*continued*)

No	Experimental wavenumber		Theoretical wavenumber				TED (<10%)
	FT-IR	FT-Raman	Scaled	I_{IR}	S_{Ra}	I_{Ra}	Assignments[a]
71			3116	12.45	35.80	0.03	νCH(96)asm
72			3120	12.29	68.64	0.06	νCH(96)asm
73			3150	7.63	139.34	0.13	νCH(96)sm
74			3153	7.38	43.19	0.04	νCH(91)asm
75			3244	1.90	61.13	0.05	νCH(97)asm

[a] ν; stretching, γ; out of plane bending, δ; in plane-bending, τ; torsion, sm; symmetric, asm; asymmetric.

Table 3
Experimental and calculated chemical shifts (ppm) of CMA2OEM.

Atom	Calculated			Experimental
	Gas	Water	Chloroform	Chloroform
C9	173.89	174.70	174.49	166.90
C15	171.46	174.16	173.33	166.60
C5	143.83	143.82	143.77	135.75
C6	135.05	136.09	135.90	126.50
C25	118.53	122.05	121.09	115.00
C24	117.21	121.41	120.14	114.00
C12	61.98	62.70	62.41	61.60
C21	34.80	35.70	35.42	36.30
C18	32.62	33.28	33.05	35.90
C1	20.36	19.81	19.98	18.20
H8	6.72	6.77	6.76	6.25
H7	6.02	6.22	6.16	5.72
H23	5.97	6.06	6.05	4.46
H19	5.32	5.37	5.37	4.46
H14	4.73	4.92	4.85	4.90
H13	3.97	4.16	4.11	4.90
H22	3.90	4.15	4.08	4.46
H20	3.34	3.76	3.62	4.46
H2	2.14	2.03	2.08	1.94
H3	2.02	2.00	2.00	1.94
H4	1.61	1.80	1.74	1.94

4.2.1. *C–N and C≡N vibrations*

The C–N stretching mode was assigned as 1368 cm^{-1} in benzamide by Pinchas et al. [13]. For CMA2OEM molecule observed bands at 1242 cm^{-1} in FT-IR and 1448 cm^{-1} in FT-Raman. The theoretically value C–N stretching vibration was computed between 1208 and 1306, 1443 cm^{-1} and this band in 1208 cm^{-1} have TED of 43%. In according to TED, this band looks coupled with CCH bending vibration. In the case of 2-amino-5-chlorobenzonitrile the strong FT-IR band at 2230 cm^{-1} was assigned to C≡N stretching vibration [14]. In title molecule the C≡N stretching mode appears in our calculation at 2247 cm^{-1} in FT-IR and it was calculated at 2353 and 2356 cm^{-1} with a composition of 91% and 92%.

4.2.2. *CH_3 and CH_2 vibrations*

The asymmetric stretch is usually observed at higher wavenumber than the symmetric stretch. The asymmetric C–H stretching mode of CH_3 is expected around 2980 cm^{-1} and symmetric C–H stretching mode of CH_3 should be at 2870 cm^{-1} from previous works in the literature [15–18]. Asymmetric stretching vibrations of CH_3 of CMA2OEM were calculated at 3120, 3090 cm^{-1} and symmetric stretching vibration was calculated at 3038 cm^{-1}. This band was observed at 2960 cm^{-1} in FT–IR and 2943 cm^{-1} in FT-Raman spectrum. These vibrations show ~97% of TED contribution suggesting that it is a pure stretching mode. Scissoring vibrations of CH_3 were calculated at 1506, 1474 and 1440 cm^{-1} with B3LYP/CC-pVDZ method and it observed 1458 and 1431 cm^{-1} in FT–IR spectrum.

The symmetric and asymmetric stretching vibrations in CH_2–C≡N groups are calculated at 3042, 3058 cm^{-1} and in between of 3097–3116 cm^{-1}, respectively. This band was recorded at 2999 cm^{-1} in FT-IR spectrum. The symmetric stretching band in O–CH_2–C=O and C=CH_2 groups are computed at 3097, 3107 cm^{-1} and at 3150 cm^{-1}. The asymmetric stretching band in this groups were calculated at 3153 and 3244 cm^{-1}.

C–O and C=O vibrations

The carbon oxygen double band is formed by $\pi - \pi$ bonding between carbon and oxygen-intermolecular hydrogen bonding, which reduces the frequencies of the C=O stretching absorption to a greater degree than does inter molecular H bonding because of the different electro negative of C and O. The bonding is not equally distributed between two atoms. C=O stretching band appears strongly in the region 1700-1800 cm^{-1} and this vibration appears in the expected range shows that it is not much affected by other vibrations. C=O stretching vibrations for CMA2OEM molecule were observed as 1720 cm^{-1} and 1774 cm^{-1} in FT-Raman spectrum and its calculated as 1744 and 1748 cm^{-1} with B3LYP/6–311++G(d,p) methods In addition, C–O stretching band in FTIR at 1161 $cm^{-1}$and its was also calculated as 1173 cm^{-1} and TED value is 37% as reported in Table 2.

4.3. *NMR analysis*

The ^{1}H NMR spectrum of CMA2OEM shows the following peaks at 6.25 and 5.72 ppm for =CH_2 olefinic protons, 4.9 ppm O–CH_2 protons, 4.46 ppm *N*–CH_2, 1.94 ppm for CH_3 protons. The calculated

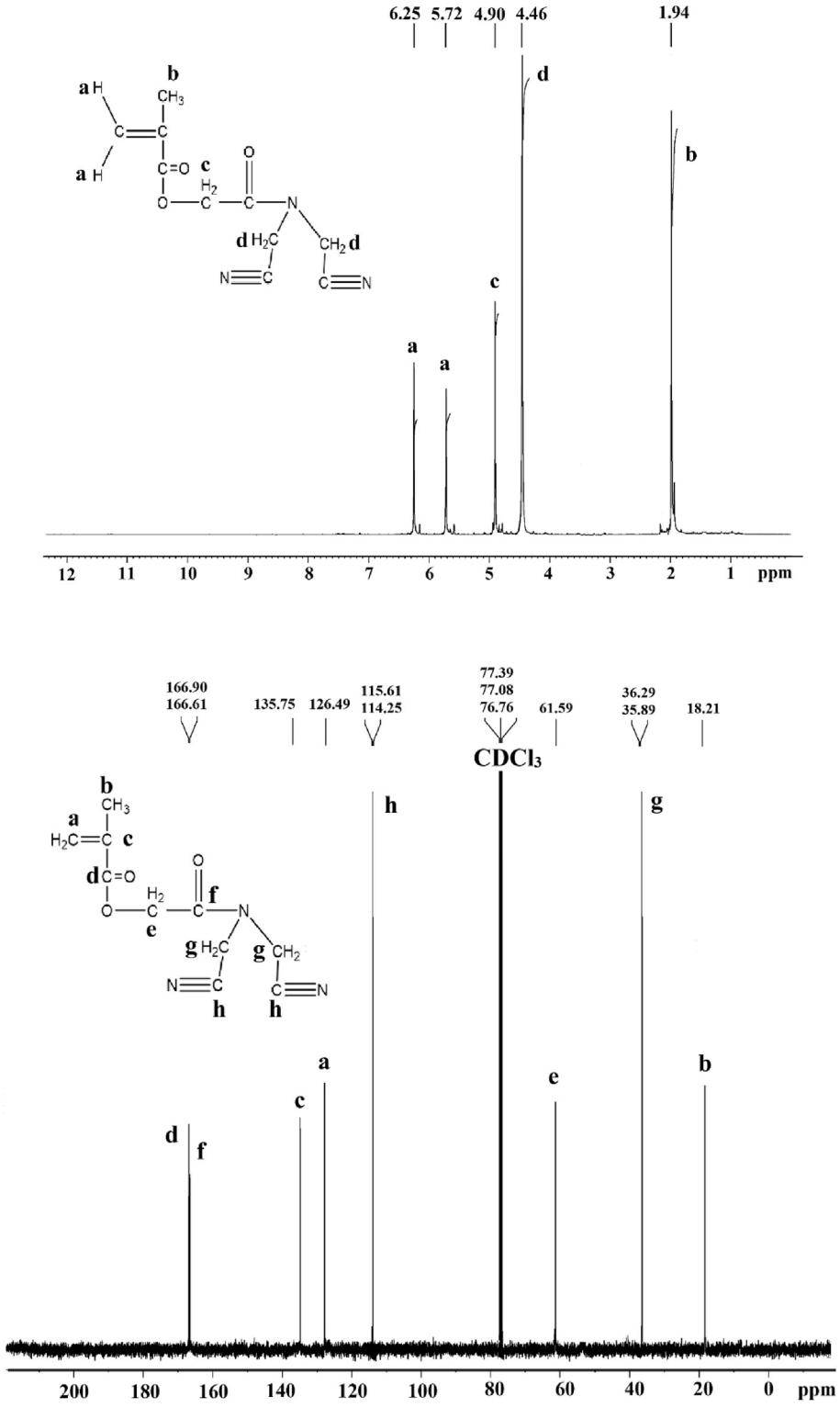

Fig. 4. ^{1}H and ^{13}C NMR spectra of theCMA2OEM in chloroform solution.

and experimental data are given in Table 3; all of H19,20,22 and 23 are expected in the same place at the ^{1}H NMR peak and the experimental data supports it. In H19 and 23, a small deviation is observed in experimental and theoretical calculations compared to H22 and 20 in similar positions. H19 and 23 are located closer to the nitrogen atom which is the electronegative atom in position. Therefore it is more affected by the nitrogen atom. In the same way, H13 is more affected by electronegative oxygen atom than H14, because of its position. ^{13}C NMR spectrum of the experimental data CMA2OEM following peaks appear; at 166.9 ppm for ester C═O, 166.6 ppm for amide C═O, 135.8 ppm for = C, 126.5 ppm for = CH olefinic, 115.6 and 114.3 ppm for N≡C, 61.6 ppm for O–CH_2, 36.3

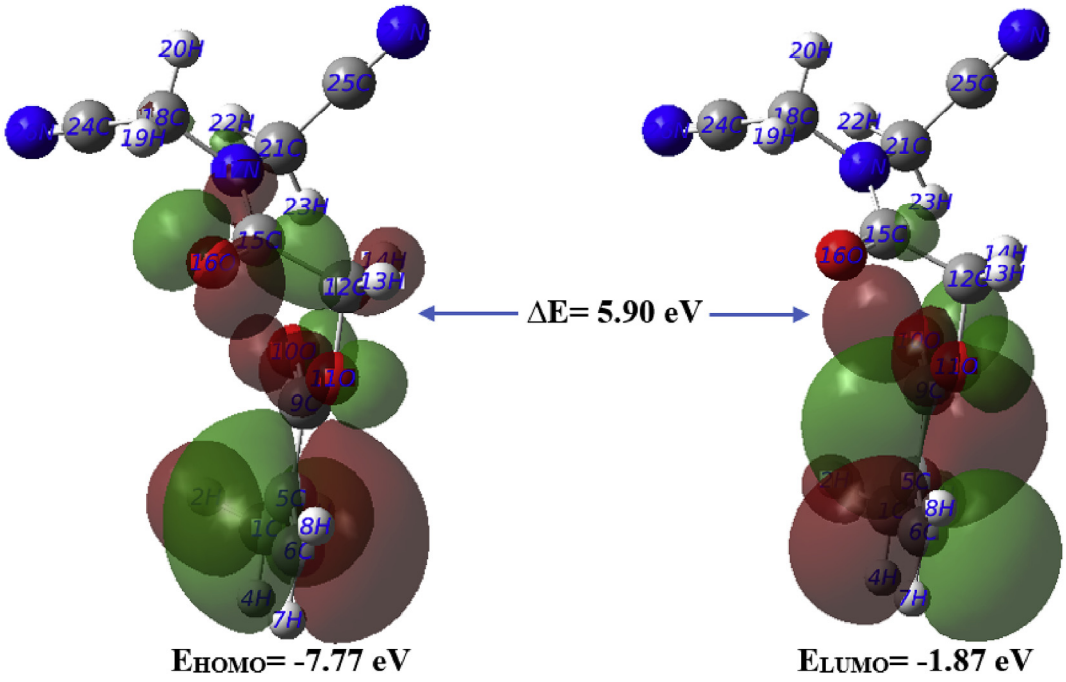

Fig. 5. The frontier molecular orbitals of theCMA2OEM for gas phase.

Table 4
The calculated energies values of CMA2OEM using by the TD-DFT/B3LYP method using 6–311++G(d,p) basis set.

C_2 symmetry	Gas	Water	Acetonitrile
E_{total} (Hartree)	−777.78868262	−777.80861450	−777.80808710
E_{total} (eV)	−21164.40784	−21164.95021	−21164.93586
E_{LUMO+1} (eV)	−1.03	−1.03	−1.03
E_{LUMO} (eV)	−1.87	−1.87	−1.87
E_{HOMO} (eV)	−7.77	−7.77	−7.77
E_{LUMO-1} (eV)	−8.08	−8.08	−8.08
$E_{HOMO-1-LUMO+1\ gap}$ (eV)	**7.05**	**7.05**	**7.05**
$E_{HOMO-LUMO\ gap}$ (eV)	**5.90**	**5.90**	**5.90**
Chemical hardness (h)	2.95	2.95	2.95
Electronegativity (χ)	−4.82	−4.82	−4.82
Chemical potential (μ)	4.82	4.82	4.82
Electrophilicity index (ω)	3.94	3.94	3.94

and 25.9 ppm for *N*–CH_2, 18.2 ppm for CH_3 carbons. When looking at experimental data; C9 and C15 are connected to an oxygen double bond which is an electronegative atom. Because of the electron density around carbons, ^{13}C NMR results in high ppm peak. This electron density may cause a small deviation between experimental and theoretical data. Likewise, C5 is affected by the electronegativity of oxygen because it is close to the oxygen position. ^{1}H and ^{13}C NMR spectrums of CMA2OEM are shown in Fig. 4 and this values are tabulated Table 3.

4.4. Frontier molecular orbitals

The energy values of HOMO and LUMO orbitals play a characteristic role in the optical and electrical attributes, it is a critical parameter [19,20]. These values are presented by TD-DFT method for CMA2OEM and are given in Fig. 5 for gas phase. The HOMO orbitals is localized in the whole of molecule except CH_2–C≡N groups and LUMO orbitals is localized in the propene groups. The energy gap of HOMO and LUMO orbitals is found to be 5.90 eV in gas phase. The values chemical hardness, chemical potential, electrophilicity index and electronegativity for CMA2OEM were also calculated and are given Table 4.

4.5. Total, partial and population density of states (DOS, PDOS and OPDOS)

Taking account of only the HOMO-LUMO orbitals may not give a real definition. In this case, neighboring orbitals also can use characterization of frontier orbitals. Therefore, the TDOS, PDOS, and OPDOS density of states [21–23] were computed and created by convoluting the molecular orbital information with Gaussian curves of unit height and the full width at half maximum of 0.3 eV using GaussSum 2.2 program [11] The main application of the OPDOS plots display the bonding, anti-bonding and nonbonding nature of the interaction of the two orbitals. Positive, negative and zero values of the OPDOS indicate a bonding, anti–bonding and nonbonding interactions, respectively [24]. These plots for CMA2OEM were drawn in Figs. S2–4. Atoms were divided into three groups as 2-oxoethyl formate, imidiasetonitrile and propene. As seen in the OPDOS diagram, some of orbital energy values of

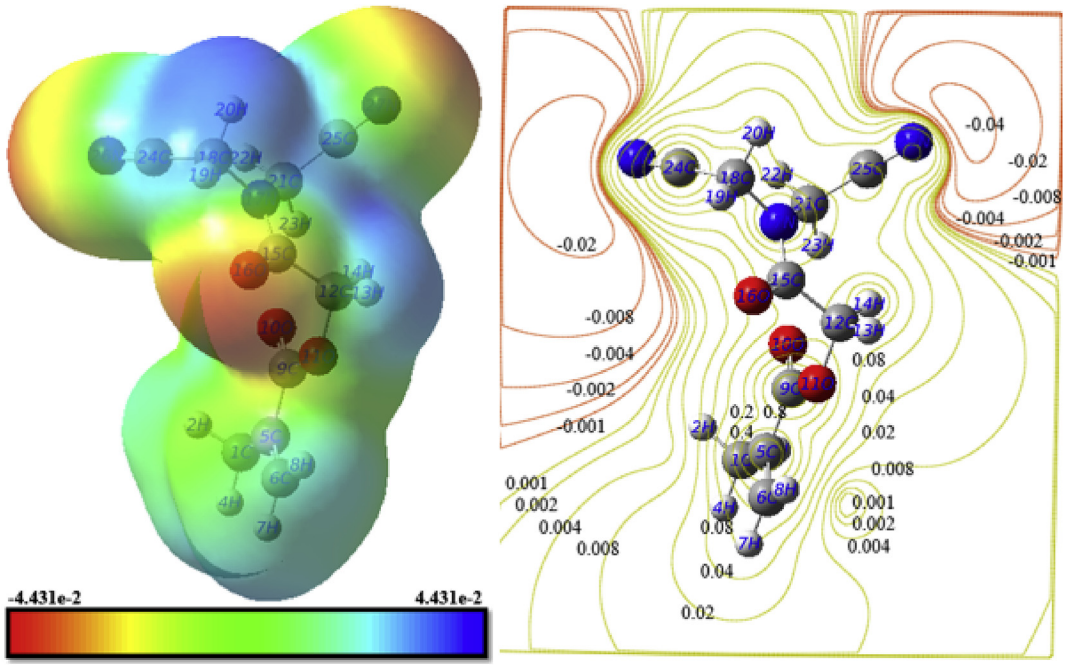

Fig. 6. Molecular electrostatic potential (MEPs) 3D and 2D contour map for CMA2OEM.

Table 5
Thermodynamic properties at different temperatures at the B3LYP/6311++G(d,p) level for CMA2OEM.

T (K)	C (cal mol^{-1} K^{-1})	S (cal mol^{-1} K^{-1})	ΔH (kcal mol^{-1})
100	28.469	91.435	2.081
150	36.607	105.341	3.810
200	44.222	117.496	5.932
250	51.598	128.602	8.427
298.15	58.574	138.640	11.176
300	58.839	139.015	11.288
350	65.833	148.920	14.506
400	72.436	158.413	18.064
450	78.551	167.536	21.940
500	84.148	176.316	26.108
550	89.242	184.769	30.545
600	93.868	192.908	35.224
650	98.075	200.749	40.123
700	101.909	208.307	45.224

Table 6
The calculated thermo dynamical parameters of CMA2OEM at 298.15 K for all forms in ground state at the B3LYP/6–311++G(d,p) level.

Symmetry group	C1
SCF energy (a.u.)	−777.78868262
Zero point vib. energy (kcal mol^{-1})	128.09206
Rotational constants (GHz)	0.74280
	0.30478
	0.27800
Specific heat, Cv (cal mol^{-1} K^{-1})	58.574
Entropy, S (cal mol^{-1}K^{-1})	138.640

interaction between selected groups, such as 2-oxoethyl formate ↔ imidiasetonitrile and 2-oxoethyl formate ↔ propene system characterized as red and blue line have anti–bonding interaction.

4.6. Molecular electrostatic potential surface

2D contour map provide predicting the interaction of different geometries [25–31]. 2D contour map and 3D molecular electrostatic potential surface for CMA2OEM were drawn and given in Fig. 6. The negative (red) regions and positive (blue) regions show electrophilic reactivity and nucleophilic reactivity, respectively. The color code maps for the title compound were predicted in between of −0.04431 (darkest red) and 0.04431a.u. (darkest blue). Fig. 6 indicates that the region around the nitrogen and oxygen atoms has the most electrophilic reactivity (red) and the hydrogen atoms have the most of nucleophilic reactivity (blue).

4.7. Thermodynamic properties

Thermodynamic parameters obtained by B3LYP/6–311++G(d,p) method at 298.15 K for CMA2OEM were tabulated in Table 5. Parameters as heat capacity at constant pressure, entropy and enthalpy changes which were calculated in the temperature range of 100–700 K varied every 50 K are presented in Table 6. There was a thermodynamic parameters enhancement with the rise of temperature because of the molecular vibrational intensity enhancement by temperature [32]. The correlation graphics of temperature dependence of thermodynamic functions for the title compound molecule are given in Fig. 7. The correlation equations between heat capacity, entropy, enthalpy changes and temperatures are fitted by quadratic formulas. The corresponding fitting equations are as follows:

$$C = 10.222 + 0.1868T - 8x10^{-5}T^2 \quad R^2 = 0.9999$$

$$S = 67.051 + 0.267T - 9x10^{-5}T^2 \quad R^2 = 0.9997$$

$$\Delta H = -1.0324 + 0.0228T + 6x10^{-5}T^2 \quad R^2 = 0.9999$$

From Fig. 7, it can be observed that these thermodynamic functions are increasing with temperature.

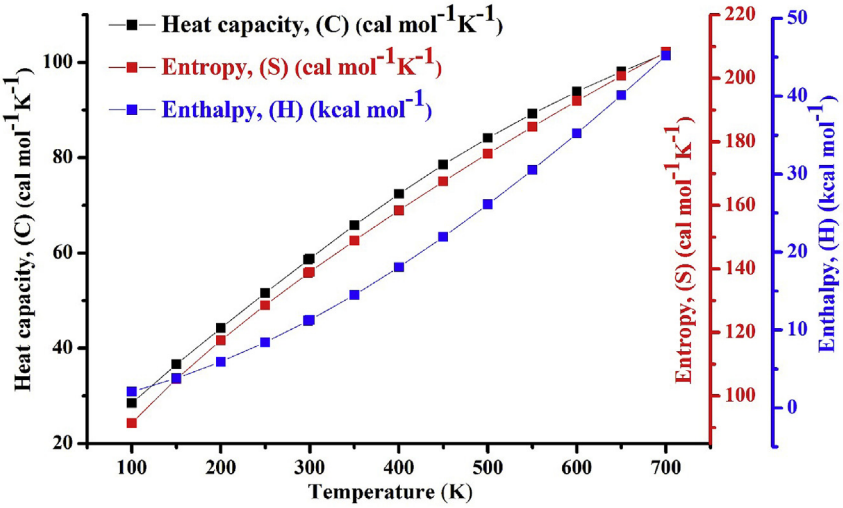

Fig. 7. The correlation graphic of heat capacity, entropy, entalpy and temperature for CMA2OEM.

5. Conclusion

In this study, newly synthesized 2- (bis (cyanomethyl) amino) -2-oxoethyl methacrylate (CMA2OEM) compound was obtained with the 2-stage reaction, and more characterized by FT-IR, FT-Raman, ^{1}H and ^{13}C NMR spectroscopy techniques. The spectra and chemical shifts of molecule were compared with the experimental values, showing a very good agreement. MEPs contour/surface, HOMO-LUMO and thermodynamic graphics were drawn in order to understand the attributes and dynamics of the molecule. The correlations between the thermodynamic parameters and temperature were drawn. Both experimental and theoretical methods showed that the monomer was successfully synthesized. The results showed that the calculated frequencies correspond to the experimental values.

Acknowledgements

This work was supported by Ahi Evran University Scientific Project Unit (BAP) with, Project No: PYO–FEN.4001.15.012.

Appendix A. Supplementary data

Supplementary data related to this article can be found at https://doi.org/10.1016/j.molstruc.2018.01.088.

References

[1] Y. Acikbas, N. Cankaya, R. Capan, M. Erdogan, C. Soykan, J. Macromol. Sci., Pure Appl. Chem. 53 (1) (2016) 18–25.
[2] S. Barral, A. Guerreiro, M.A. Villa-Garcıa, M. Rendueles, M. Dıaz, S. Piletsky, React. Funct. Polym. 70 (2010) 890–899.
[3] J.M. Cervantes-Uc, J.V. Cauich-Rodriguez, W.A. Herrera-Kao, H. Vazquez-Torres, A. Marcos-Fernandez, Polym. Degrad. Stabil. 93 (2008) 1891–1900.
[4] S.E. Kudaibergenov, A. Larisa, A. B Imend Ina, M.G. Yashkarova, J. Macromol. Sci. 44 (2007) 899–912.
[5] N. Cankaya, K. Demirelli, J. Chem. Soc. Pakistan 33 (6) (2011) 884–892.
[6] C. Soykan, A. Şahan, F. Yakuphanoglu, J. Macromol. Sci. 48 (2011) 169–176.
[7] http://cccbdb.nist.gov/vsfx.asp.
[8] J. Baker, A.A. Jarzecki, P. Pulay, Direct scaling of primitive valence force constants: an alternative approach to scaled quantum mechanical force fields, J. Phys. Chem. A102 (1998) 1412–1424.
[9] M.E. Casida, J.M. Seminario (Eds.), Recent Developments and Applications of Modern Density Functional Theory, Theoretical and Computational Chemistry, vol. 4, Elsevier, Amsterdam, 1996, p. 391.
[10] R. Ditchfield, Chem. Phys. 76 (1972) 5688–5691.
[11] N.M. O'Boyle, A.L. Tenderholt, K.M. Langner, J. Comput. Chem. 29 (2008) 839–845.
[12] M.J. Frisch, et al., Gaussian 09, Revision A.1, Gaussian, Inc., Wallingford, CT, 2009.
[13] S. Pinchas, D. Samuel, M. Weiss-Broday, J. Chem. Soc. 1688 (1961).
[14] V. Krishnakumar, S. Dheivamalar, Spectrochim. Acta 71A (2008) 465.
[15] V. Krishnakumar, V. Balachandran, T. Chithambarathanu, Spectrochim. Acta 62A (2005) 918.
[16] V. Krishnakumar, R. John Xavier, Indian J. Pure Appl. Phys. 41 (2003) 597.
[17] V. Krishnakumar, V.N. Prabavathi, Spectrochim. Acta Part A (71) (2008) 449.
[18] F. Weinhold, C.R. Landıs, Chemistry Education Research and Practice in Europe 2 (2) (2001) 91–104.
[19] I. Fleming, Frontier Orbitals and Organic Chemical Reactions, Wiley, London, 1976.
[20] K. Fukui, Science 218 (1982) 747–754.
[21] R. Hoffmann, , Solids and Surfaces: a Chemist's View of Bonding in Extended Structures, VCH Publishers, New York, 1988.
[22] T. Hughbanks, R. Hoffmann, J. Am. Chem. Soc. 105 (1983) 3528.
[23] J.G. Małecki, Polyhedron 29 (2010) 1973.
[24] H.O. Kalinowski, S. Berger, S. Braun, Carbon–13 NMR Spectroscopy, John Wiley and Sons, Chichester, 1988.
[25] E. Scrocco, J. Tomasi, Adv. Quant. Chem. 11 (1978) 115–121.
[26] C. Muñoz-Caro, A. Niño, M.L. Sement, J.M. Leal, S. Ibeas, J. Org. Chem. 65 (2000) 405–410.
[27] P. Politzer, K.C. Daiker, The Force Concept in Chemistry, Van Nostrand Reinhold Co, 1981.
[28] P. Politzer, P.R. Laurence, K. Jayasuriya, in: J. McKinney, structure activity correlation in mechanism studies and predictive toxicology, Special Issue of Environ. Health Perspect., vol. 61, 1985, p. 191.
[29] P. Politzer, J.S. Murray, in: D.L. Protein, R. Beveridge, R. Lavery (Eds.), Theoretical Biochemistry and Molecular Biophysics: a Comprehensive Survey, vol. 2, Adenine Press, Schenectady, NY, 1991, pp. 165–191.
[30] E. Scrocco, J. Tomasi, Topics in Current Chemistry, vol. 42, Springer Verlag, Berlin, 1973.
[31] P. Politzer, D.G. Truhlar (Eds.), Chemical Applications of Atomic and Molecular Electrostatic Potentials, Plenum Press, NY, 1981.
[32] J.B. Ott, J. Boerio-Goates, Chemical Thermodynamics: Advanced Applications, Calculations from Statistical Thermodynamics, Academic Press, 2000.